

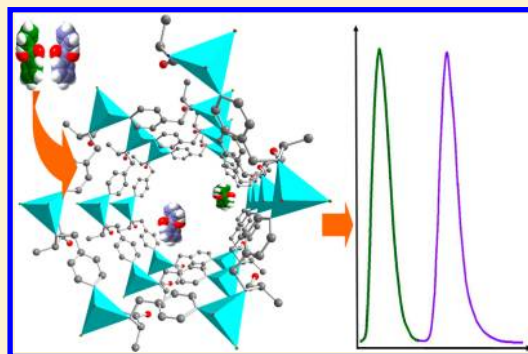
# High-Performance Liquid Chromatographic Enantioseparation of Racemic Drugs Based on Homochiral Metal–Organic Framework

Xuan Kuang,<sup>†</sup> Yu Ma,<sup>†</sup> Hao Su, Jine Zhang, Yu-Bin Dong, and Bo Tang\*

College of Chemistry, Chemical Engineering and Materials Science, Collaborative Innovation Center of Functionalized Probes for Chemical Imaging, Key Laboratory of Molecular and Nano Probes, Ministry of Education, Shandong Normal University, Jinan 250014, People's Republic of China

## Supporting Information

**ABSTRACT:** Homochiral metal–organic frameworks with fine-tuned pore sizes/walls and large surface areas are promising porous materials for enantioseparation considering the traditional zeolite molecular sieves have no chirality. Using enantiopure pyridyl-functionalized salen [(*N*-(4-Pyridylmethyl)-*L*-leucine·HBr)] as a starting material, we have prepared a noninterpenetrated three-dimensional homochiral metal organic framework {[ZnLBr]·H<sub>2</sub>O}<sub>*n*</sub>, which was further used as a chiral stationary phase for high-performance liquid chromatography to enantioseparate racemic drugs, showing excellent performances in enantioseparation of drugs. The metal–organic framework can be regarded as a novel molecular sieve-like material with a chiral separation function based on the relative sizes of the chiral channels and the resolved molecules.



Separation of enantiomers has become an increasingly significant task in stereochemistry as well as in preparation of biologically active compounds, in particular, drugs,<sup>1–5</sup> because pure enantiomers may profoundly differ in biological interactions, pharmacology and toxicity. In many cases, the opposite enantiomers show unwanted side effects or even toxic effects.<sup>6–8</sup> Chromatographic techniques based on chiral stationary phases (CSPs) have become an indispensable part of drug discovery for chiral analyses and preparation.<sup>9–12</sup> The traditional porous materials, such as zeolite molecular sieves, possess high specific surface areas, uniform pore structures and pore sizes, but the preparation of these materials with optical activity is still very challenging,<sup>13–19</sup> and the local chirality is often destroyed during the removal of templates or activation.<sup>18,19</sup> Emerging chiral metal–organic frameworks (MOFs), as new types of porous adsorbent materials, have great potential as CSPs for chromatographic enantioseparation, due to their large specific surface areas, controllable synthesis and flexibility of the pore sizes.<sup>20–25</sup> However, the research of chiral MOFs for enantioseparations has mainly focused on selective adsorption and resolution of enantiomers in the mixture on the adsorbents for evaluating their potential separation performance.<sup>21,22,26–30</sup> To the best of our knowledge, these homochiral MOFs rarely were adopted in traditional chromatographic techniques<sup>31–35</sup> and used for molecular sieve-like enantioseparation. Combining the advantages of the traditional molecular sieve materials and the emerging chiral MOFs, we synthesized a novel molecular sieve-like homochiral MOF, {[ZnLBr]·H<sub>2</sub>O}<sub>*n*</sub> (1·H<sub>2</sub>O), assembled by a enantiopure pyridyl-functionalized salen ligand, [*N*-(4-Pyridylmethyl)-*L*-leucine·HBr] (1-HL). 1·H<sub>2</sub>O, showing non-interpenetrated 3D porous frameworks, which was then used in

enantioseparation based on the relative sizes of the chiral channels and the resolved molecules

## EXPERIMENTAL SECTION

**Materials and General Procedures.** (+)-ibuprofen, (±)-ibuprofen; (–)-1-phenyl-1-propanol, (±)-1-phenyl-1-propanol; (–)-benzoin, (±)-benzoin; DL-ketoprofen; (±)-naproxen and HPLC grade *n*-hexane and 2-propanol (IPA) were purchased from Sigma-Aldrich (Shanghai, China). (+)-1-phenylethylamine and (±)-phenylethylamine were purchased from TCI (Shanghai, China) Chemical Industry Co., Ltd. Zinc acetate, *L*-leucine, *D*-leucine, sodium borohydride, sodium carbonate and 4-pyridinecarboxaldehyde were obtained from Aladdin (Aladdin Chemistry Co. Ltd., Shanghai, China). Ultrapure water (18.2MU cm) was obtained from a Water Pro Water Purification System (Labconco Corporation, Kansas City, USA). Unless otherwise stated, all chemicals and reagents used were at least of analytical grade and as received without further purification.

**Apparatus.** Elemental analyses were determined on a Perkin-Elmer Model 2400 analyzer. The FT-IR (KBr pellet) spectrum was recorded (400–4000 cm<sup>–1</sup> region) on a Nicolet Magna 750 FT-IR spectrometer. The chemical shifts were reported in  $\delta$  relative to TMS. Thermogravimetric analyses (TGA) were carried out under flowing nitrogen at a heating rate of 10 °C·min<sup>–1</sup> on a STA449C integration thermal analyzer. Powder X-ray Diffraction (PXRD) patterns were

Received: November 12, 2013

Accepted: December 31, 2013

Published: December 31, 2013

measured at room temperature (298 K) on a Bruker SMART APEX CCD-based diffractometer (Cu K $\alpha$  radiation,  $\lambda = 1.5418$  Å). The solid state CD spectra were recorded on a J-815 spectropolarimeter (Jasco, Japan). The SEM images were recorded on a FEI QUANTA FEG250 scanning electron microscope at 15.0 kV.

**Synthesis of Ligands *l*-HL and *d*-HL.** The ligand [(*N*-(4-Pyridylmethyl)-*l*-leucine·HBr, *l*-HL)] was synthesized according to the literature.<sup>36,37</sup> Typically, a solution of 4-pyridinecarboxaldehyde (2.14 g, 20 mmol) in MeOH (10 mL) was added dropwise to a solution of *l*-leucine (2.7 g, 20 mmol) and sodium carbonate (1.06 g, 10 mmol) in water (40 mL). The mixture was stirred at room temperature for 2 h, and then cooled in an ice bath. A solution of sodium borohydride (0.91 g, 24 mmol) in water (10 mL) was added. The mixture was stirred for 1 h and acidified to pH = 5 by adding hydrobromic acid. The solution was stirred for another 2 h and then was evaporated to dryness. The solid (residue) was extracted with MeOH (10 mL), and the extract was evaporated to get a white powder. Yield: 3.4 g (70%). Elemental analysis for C<sub>12</sub>H<sub>19</sub>BrN<sub>2</sub>O<sub>2</sub>: Calcd: C, 47.54%; H, 6.32%; N, 9.24%. Found: C, 47.52%; H, 6.33%; N, 9.23%. IR (KBr, cm<sup>-1</sup>):  $\gamma_{\text{O-H}}$ , 3430;  $\gamma_{\text{C=O}}$ , 1577 ( $\nu_{\text{as}}$ ) and 1385 ( $\nu_{\text{s}}$ ). <sup>1</sup>H NMR (DMSO-*d*<sub>6</sub> 300 MHz): -CH<sub>3</sub> (0.81, d, 3H), -CH<sub>3</sub> (0.84, d, 3H), -CH (1.76, m, 1H), -CH<sub>2</sub> (1.57, t, 2H), -CH (3.37, t, 1H), -NH (4.28, m, 1H), -CH<sub>2</sub> (3.98, dd, 2H), py-H (7.33, d, 2H), py-H (8.49, d, 2H).

The ligand [(*N*-(4-Pyridylmethyl)-*D*-leucine·HBr, *d*-HL)] was prepared exactly as *l*-HL, except *D*-leucine was used instead of *l*-leucine. Yield, 3.3 g, 68%. Calcd for C<sub>12</sub>H<sub>19</sub>BrN<sub>2</sub>O<sub>2</sub>: C, 47.54%; H, 6.32%; N, 9.24%. Found: C, 47.52%; H, 6.33%; N, 9.23%. IR (KBr, cm<sup>-1</sup>):  $\gamma_{\text{O-H}}$ , 3425;  $\gamma_{\text{C=O}}$ , 1575 ( $\nu_{\text{as}}$ ) and 1388 ( $\nu_{\text{s}}$ ). <sup>1</sup>H NMR (DMSO-*d*<sub>6</sub> 300 MHz): -CH<sub>3</sub> (0.81, d, 3H), -CH<sub>3</sub> (0.84, d, 3H), -CH (1.76, m, 1H), -CH<sub>2</sub> (1.57, t, 2H), -CH (3.37, t, 1H), -NH (4.28, m, 1H), -CH<sub>2</sub> (3.98, dd, 2H), py-H (7.33, d, 2H), py-H (8.49, d, 2H).

**Synthesis of Homochiral 1·H<sub>2</sub>O and 2·H<sub>2</sub>O.** Homochiral porous 1·H<sub>2</sub>O was synthesized by the diffusion of methanol vapor into a water solution of *l*-HL (0.45 g, 2 mmol) and Zn(CH<sub>3</sub>COO)<sub>2</sub>·2H<sub>2</sub>O (0.22 g, 1 mmol) at room temperature for 3 days. The colorless rod-shaped crystals were collected by filtration and washed with methanol/H<sub>2</sub>O (1:1, *v/v*) for several times, yield: 0.29 g, 75%. **1** was obtained by evacuating 1·H<sub>2</sub>O under vacuum at 150 °C for 24 h. Elemental analysis for C<sub>12</sub>H<sub>19</sub>N<sub>2</sub>O<sub>3</sub>ZnBr (%) Calcd: C, 37.48%; H, 4.98%; N, 7.28%. Found: C, 37.47%; H, 4.50%; N, 7.27%. Main IR (KBr, cm<sup>-1</sup>):  $\gamma_{\text{O-H}}$ , 3430;  $\gamma_{\text{C=O}}$ , 1587 ( $\nu_{\text{as}}$ ) and 1389 ( $\nu_{\text{s}}$ ).

The homochiral porous 2·H<sub>2</sub>O was synthesized exactly as **1**·H<sub>2</sub>O, except *d*-HL was used instead of *l*-HL. Elemental analysis for C<sub>12</sub>H<sub>19</sub>N<sub>2</sub>O<sub>3</sub>ZnBr (%) Calcd: C, 37.48%; H, 4.98%; N, 7.28%. Found: C, 37.47%; H, 4.50%; N, 7.27%. Main IR (KBr, cm<sup>-1</sup>):  $\gamma_{\text{O-H}}$ , 3420;  $\gamma_{\text{C=O}}$ , 1587 ( $\nu_{\text{as}}$ ) and 1387 ( $\nu_{\text{s}}$ ).

## RESULTS AND DISCUSSION

**Single-Crystal X-ray Structure of **1**.** Single-crystal X-ray structural analysis revealed that 1·H<sub>2</sub>O crystallizes in the chiral space group *P*61 and exhibits noninterpenetrated three-dimensional porous frameworks. The asymmetric unit of the framework contains one Zn(II) ion, one L ligand, a bromine atom and a guest water molecule. Each metal ion exhibits a highly distorted trigonal bipyramid coordination geometry completed by two carboxylate oxygen atoms (O1 and O2B), two nitrogen atoms (N1 and N2A) from three different L

ligands and a bromine atom (Br1) (Figure 1). The L ligand exhibits a quadridentate bridging coordination mode. Each

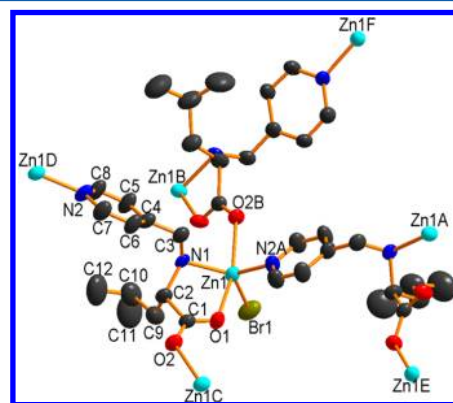


**Figure 1.** Local coordination environments of the Zn center and the chiral ligands in compound 1·H<sub>2</sub>O. Hydrogen atoms are omitted for clarity, and the symmetry codes are (A)  $1 + x - y, 1 + x, 0.16667 + z$ ; (B)  $-x + y, 1 - x, -0.33333 + z$ ; (C)  $1 - y, 1 + x - y, 0.33333 + z$ ; (D)  $-1 + y, -x + y, -0.16667 + z$ ; (E)  $1 - x, 2 - y, 0.5 + z$ ; (F)  $1 - x, 2 - y, -0.5 + z$ .

carboxylate group serves as a syn-anti bridge between metal ions, with the Zn...Zn distances being 5.314(1) Å, leading to a 1D coordination chain. Then the chains are further connected by the L ligands through the pyridine nitrogen to a 3D framework and, simultaneously, a 1D helix channel formed along the *c* direction (Figure 2a). The helix channels are

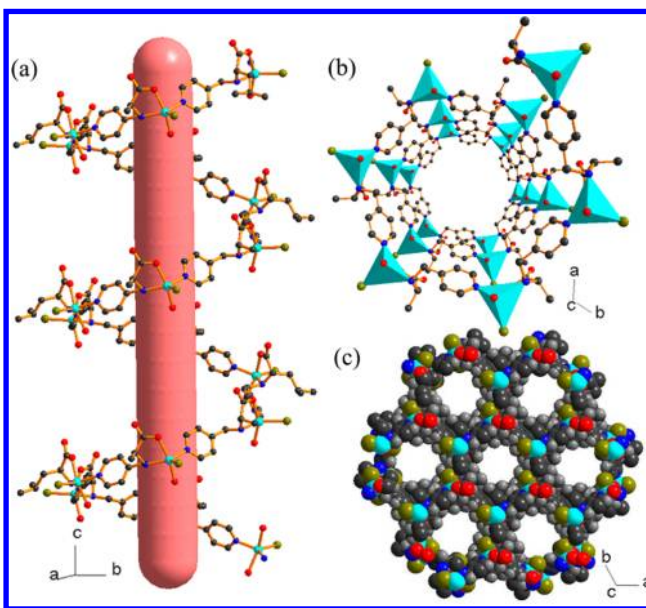


**Figure 2.** (a) Perspective view of a single helical chain in 1·H<sub>2</sub>O. (b) View down a single helical chain from the *c* direction. (c) Space-filling diagram of the 3D network of 1·H<sub>2</sub>O (Zn light blue, C gray, O red, N dark blue, Br yellow, H light gray).

occupied by the guest water molecules, which weakly H-bonded to the Br atom (3.4 Å) on the wall of the channel. The dimensions of the hexagons windows of 1·H<sub>2</sub>O are about 12 Å (9.8 Å when considering van der Waals radii) (Figure 2b,c).<sup>28,38,39</sup> To better elucidate the 3D network, taking both the crystallography independent Zn(II) and the L ligand as 3-connected nodes, the integral structure exhibits an *etd* uninodal



topology, which is different from the metal–organic framework previously reported with a similar salen ligand.<sup>36</sup> The Schläfli symbol is (8<sup>3</sup>). PLATON calculations show that the total effective free voids is 40.1%. The solid-state circular dichroism (CD) spectrum of 1·H<sub>2</sub>O and its enantiomer, 2·H<sub>2</sub>O, exhibited an obvious opposite cotton effect at 240 nm, which suggested the homochirality of 1·H<sub>2</sub>O (Supporting Information, Figure S1).

**Characterization of 1.** As known to all, the ideal materials as the CSPs of HPLC must possess not only homochirality and specific porous properties (e.g., pore size, pore volume, pore surface et al.) but also high stability in liquid phase under high pressure.<sup>40</sup> To further estimate the possibility of this homochiral MOF as a CSP of HPLC, its stability has been investigated. The thermogravimetric analyses (TGA) indicated that the framework of 1·H<sub>2</sub>O was thermally stable up to 270 °C (Supporting Information, Figure S2), whereas the crystallinity can be retained by the suggestion of PXRD (Supporting Information, Figure S3). The well-defined rod crystal of 1 was characterized by SEM with about 12 μm in length and 4 μm in width (Figure 3). Particle size distribution of 1 indicated the

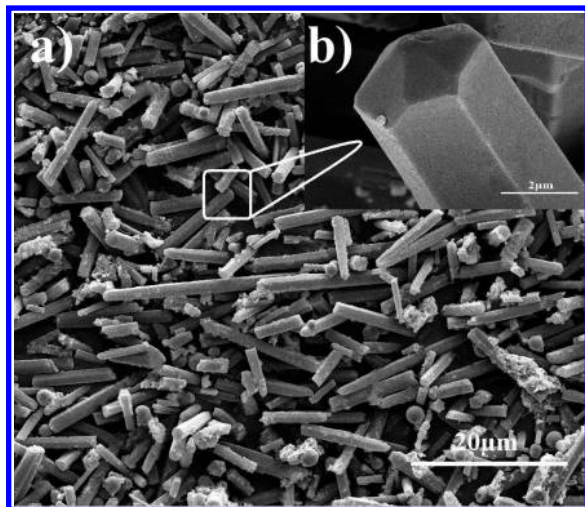


**Figure 3.** SEM images of 1 packing for HPLC with different magnifications: (a) (×2000) and (b) (×20 000).

mean particle size was around 7 μm (Supporting Information, Figure S4). In addition, both 1·H<sub>2</sub>O and 1 are insoluble in water and common organic solvents like methanol, ethanol, tetrahydrofuran, dimethylformamide and dimethyl sulphoxide.

**HPLC Separation of Drugs on 1.** The packed column for HPLC was prepared by loading the suspension of 1 (2.3 g) in methanol into a 10 cm long ×4.6 mm i.d. stainless steel column under 5000 psi. The performance of the CSP was first evaluated by enantioseparation of (±)-ibuprofen with carboxylic groups, which has been widely used for treatment of diseases such as osteoarthritis and rheumatoid arthritis, but (+)-ibuprofen has been reported to be 160 times more active than its antipode.<sup>41,42</sup> The minimum kinetic diameter (MKD) of ibuprofen is 7.4 Å, which is less than the aperture size of 1 (9.8 Å). As expected, (±)-ibuprofen was successfully resolved and baseline separated on the CSP with hexane/isopropanol (IPA) (optimized *v/v* = 95:5) as the mobile phase at a flow rate of 1 mL·min<sup>-1</sup> at 25 °C (Figure 4a). The high-resolution enantioseparation with a good selectivity factor ( $\alpha$  = 2.4) and chromatographic resolution ( $R_s$  = 4.1) was achieved only within

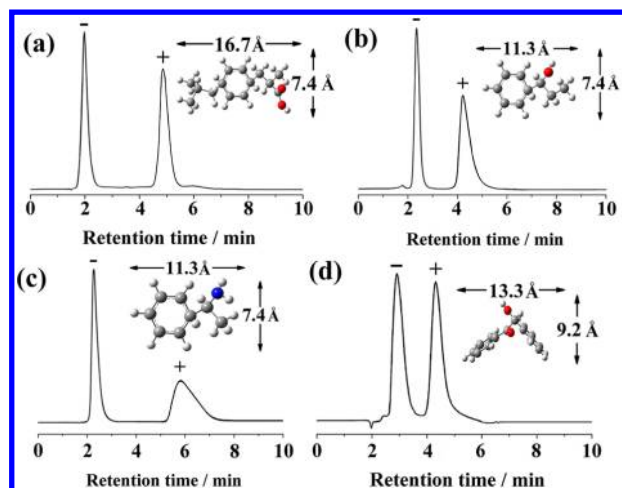


**Figure 4.** HPLC enantioseparation of racemates on the packed 1 column (10 cm long ×4.6 mm i.d.): (a) (±)-ibuprofen, (b) (±)-phenyl-1-propanol, (c) (±)-phenylethylamine and (d) (±)-benzoin at 25 °C. Inserted molecular models with the lowest energy and the sizes correspond to the MKDs considered van der Waals radii, obtained from Gaussian 03.

6 min, and the elution sequence was left-handed and right-handed. It is worth pointing out that the mobile phase composition can significantly affect the retention, resolution and selectivity.

Considering the influence of different functional groups on traditional CSPs, two racemates, (±)-1-phenyl-1-propanol with a hydroxyl group and (±)-1-phenylethylamine with an amino group, which have the same MKD as ibuprofen, were selected for comparison. Similarly, (±)-1-phenyl-1-propanol and (±)-1-phenylethylamine can also be baseline separated on the CSP with hexane/isopropanol (optimized *v/v* = 98:2 and *v/v* = 99:1, respectively) as the mobile phase. (±)-1-Phenyl-1-propanol was efficiently separated with a good selectivity factor ( $\alpha$  = 1.7) and resolution ( $R_s$  = 2.5) in a short time (within 6 min) (Figure 4b). In addition, the backpressure in the system is 7 MPa. The long retention time of (+)-1-phenylethylamine suggested that its interaction with the framework was stronger (Figure 4c). Interestingly, the elution sequence of each racemate on the 1 packed column was followed in the same order, left-handed always before right-handed.

As mentioned above, 1 possessed chiral helical channels with the aperture size of ~9.8 Å. The size covers the MKDs of all tested enantiomer pairs (7.4 Å). On this basis, we speculate that (i) these molecules are able to enter and readily go through the chiral channels. In addition, these molecules also interact with the host framework in hydrogen bonding,  $\pi$ – $\pi$  stacking, hydrophobic interaction, van der Waals forces or dipole–dipole interactions. However, they interact differently with the framework in view of the difference in the structures and shapes of these molecules; (ii) the good resolution and selectivity toward the same size enantiomer pairs with different functional group may originate from the molecular sieving effect of 1.

To show the molecular sieving effect of 1, we first used the packed 1 column for HPLC enantioseparation of (±)-benzoin, whose MKD of 9.2 Å is smaller than the MKD of chiral channels of 1 (~9.8 Å), but larger than the MKD of those aforementioned racemates. As shown in Figure 4d, the CSP also gave baseline separation using hexane/isopropanol

(optimized  $v/v = 99/1$ ) as the mobile phase at a flow rate of 1 mL·min<sup>-1</sup>. Then, we chose DL-ketoprofen and (±)-naproxen as targets owing to their MKDs of 9.4 and 9.7 Å, respectively, being close to the chiral channels of **1** (~9.8 Å). As a result, the pairs all coeluted, and the elution appeared with less retention time than those resolved enantiomers, indicating no separation for the pair compounds (Supporting Information, Figure S5). Previous study showed that MOF of MIL-53 type exhibited small reversible flexible deformations from narrow pores to wide pores in the order of 2–4% under high pressure.<sup>43–46</sup> However, the failure of **1** to resolve DL-ketoprofen or (±)-naproxen means that the framework of **1** should be rigid and stable, which was confirmed by the fact that the recycled **1** still retained its crystallinity after more than ten runs of separation in HPLC (Supporting Information, Figure S3).

On the basis of the above discussion, we question whether the enantioselectivity of **1** comes from its chiral channels. Then we soaked the crystals of **1** in a methanol solution containing (–)-benzoin and (+)-ketoprofen for 6 days at 25 °C, respectively. The soaked crystals were washed repeatedly with methanol to remove the drug molecules adsorbed on the external surfaces of the crystals and then tested by <sup>1</sup>H NMR spectroscopy. Not surprisingly, only (–)-benzoin was incorporated (Figures 5 and 6). These results clearly indicate a critical

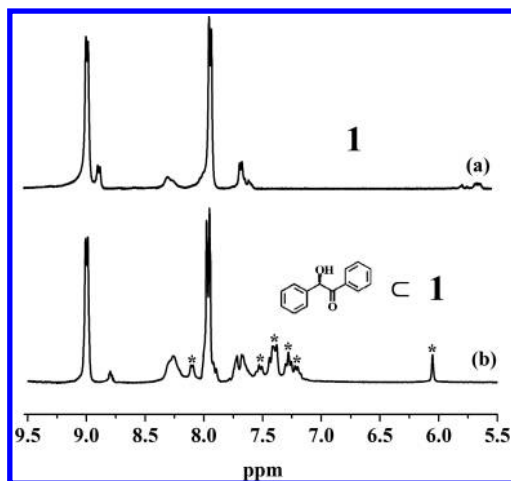


**Figure 5.** <sup>1</sup>H NMR spectra (300 MHz, DMSO-*d*<sub>6</sub>, 25 °C) of (a) **1**, (b) **1** were impregnated in a methanol solution containing (–)-benzoic. The signals marked by an asterisk correspond to the encapsulated (–)-benzoic ( $\delta$  8.09, 7.51, 7.38, 7.26, 7.20, 6.05 ppm).

size around 9.2 to 9.4 Å associated with the packed **1** column. In other words, the packed **1** column will not function well for enantioseparation when the resolved molecules are larger than 9.2 to 9.4 Å, thus demonstrating a molecular sieve-like behavior. Despite the number of tested samples for enantioseparation was limited, we can conclude that the synthesized chiral molecular sieve is capable to be used as a CSP in the separation of racemates.

**Effect of the Analyte Mass.** To examine the loading capacity of the CSP without compromising resolution, a loading test was carried out using different injection masses. Even when the loading was increased from 4.0 to 20 µg of each racemate, (±)-ibuprofen, (±)-1-phenylethylamine, (±)-1-phenyl-1-propanol or (±)-benzoin can still achieve baseline resolution as the mobile phase at a flow rate of 1 mL·min<sup>-1</sup> at 25 °C (Figure 7). Besides, the chromatographic peak area of

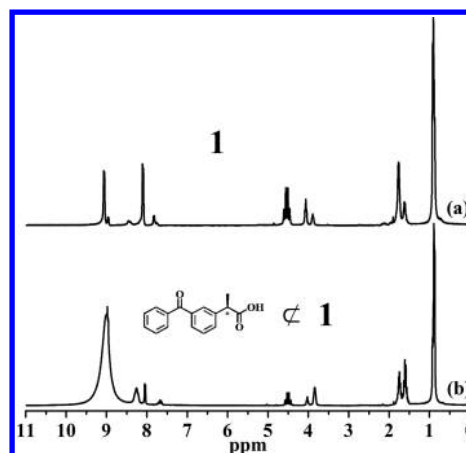


**Figure 6.** <sup>1</sup>H NMR spectra (300 MHz, DMSO-*d*<sub>6</sub>, 25 °C) of (a) **1**, (b) **1** were impregnated in a methanol solution containing (+)-ketoprofen. (+)-ketoprofen was not incorporated.

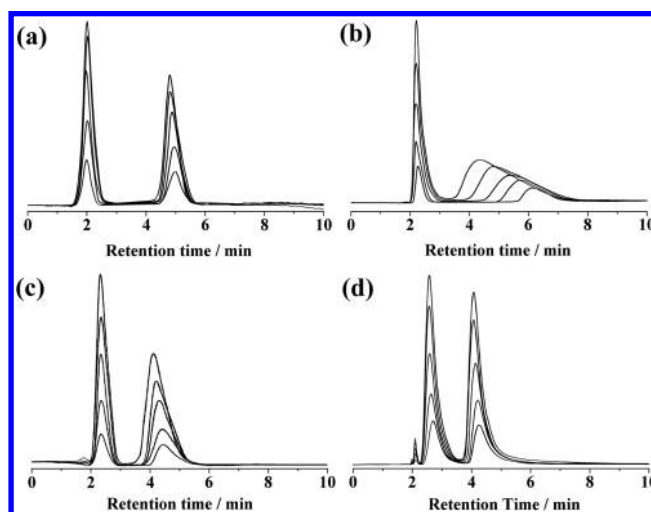


**Figure 7.** Effect of injected mass of (a) (±)-ibuprofen (Hexane/IPA = 95/5  $v/v$ ), (b) (±)-phenylethylamine (Hexane/IPA = 99/1  $v/v$ ), (c) (±)-1-phenyl-1-propanol (Hexane/IPA = 98/2  $v/v$ ) and (d) (±)-benzoin (Hexane/IPA = 99/1  $v/v$ ) on chromatograms. Injected mass: 4 µg (2 µL, 2 g L<sup>-1</sup>), 8 µg (4 µL, 2 g L<sup>-1</sup>), 12 µg (6 µL, 2 g L<sup>-1</sup>), 16 µg (8 µL, 2 g L<sup>-1</sup>), 20 µg (10 µL, 2 g L<sup>-1</sup>).

each single antipode rises linearly with the increase of the injected mass (Supporting Information, Figure S6). It was also evident that the retention time of the enantiomer for 1-phenylethylamine became closer with increasing injection mass from 4.0 to 20 µg, although achieving baseline resolution. The result may be due to stronger hydrogen bonding between amino-groups of phenylethylamine and NH groups of **1**.

## CONCLUSIONS

In summary, we have presented a new 3D rigid and stable homochiral metal–organic framework **1** with an *etd* topology for use as CSP in HPLC to enantioseparate various racemic drugs, showing molecular sieve-like performance and independence of the functional groups of resolved molecules.

## ASSOCIATED CONTENT

### Supporting Information

CIF files, single-crystal X-ray structure determination and asymmetric unit in **1**·H<sub>2</sub>O, crystal data and structure

refinement for 1-H<sub>2</sub>O, selected bond lengths [Å] and angles [deg] for 1-H<sub>2</sub>O, CD spectra for MOF1 and MOF2, TGA curves of synthesized 1-H<sub>2</sub>O and evacuated 1-H<sub>2</sub>O, PXRD patterns and results of chromatographic experiments. This material is available free of charge via the Internet at <http://pubs.acs.org>.

## AUTHOR INFORMATION

### Corresponding Author

\*B. Tang. E-mail: [tangb@sdnu.edu.cn](mailto:tangb@sdnu.edu.cn). Tel: (86)531 86180010. Fax: (86)531 86180017.

### Author Contributions

†Two authors contributed the same and are co-first authors.

### Notes

The authors declare no competing financial interest.

## ACKNOWLEDGMENTS

This work was supported by 973 Program (2013CB933800, 2012CB821705), National Natural Science Foundation of China (21227005, 21390411, 91313302, 21035003, 21205072) and Program for Changjiang Scholars and Innovative Research Team in University.

## REFERENCES

- (1) Itoh, J.; Fuchibe, K.; Akiyama, T. *Angew. Chem., Int. Ed.* **2006**, *45*, 4796–4798.
- (2) Gedrich, K.; Senkovska, I.; Baburin, I. A.; Mueller, U.; Trapp, O.; Kaskel, S. *Inorg. Chem.* **2010**, *49*, 4440–4446.
- (3) Vaidhyanathan, R.; Bradshaw, D.; Rebilly, J. N.; Barrio, J. P.; Gould, J. A.; Berry, N. G.; Rosseinsky, M. J. *Angew. Chem., Int. Ed.* **2006**, *45*, 6495–6499.
- (4) Davis, A. V.; Fiedler, D.; Ziegler, M.; Terpin, A.; Raymond, K. N. *J. Am. Chem. Soc.* **2007**, *129*, 15354–15363.
- (5) Liu, T.; Liu, Y.; Xuan, W.; Cui, Y. *Angew. Chem., Int. Ed.* **2010**, *49*, 4121–4124.
- (6) Li, J. R.; Sculley, J.; Zhou, H. C. *Chem. Rev.* **2012**, *112*, 869–932.
- (7) Nickerl, G.; Henschel, A.; Grunker, R.; Gedrich, K.; Kaskel, S. *Chem. Ing. Tech.* **2011**, *83*, 90–103.
- (8) Chankvetadze, B.; Blaschke, G. *J. Chromatogr. A* **2001**, *906*, 309–363.
- (9) Inagaki, S.; Min, J. Z.; Toyooka, T. *Anal. Chem.* **2008**, *80*, 1824–1828.
- (10) Sekhon, B. S. *Int. J. ChemTech Res.* **2010**, *2*, 1584–1594.
- (11) Ng, S. C.; Chen, L.; Zhang, L. F.; Ching, C. B. *Tetrahedron Lett.* **2002**, *43*, 677–681.
- (12) Zhang, Y.; Wu, D. R.; Wang-Iverson, D. B.; Tymiak, A. A. *Drug Discovery Today* **2005**, *10*, 571–577.
- (13) Morris, R. *Top. Catal.* **2010**, *53*, 1291–1296.
- (14) Morris, R. E.; Bu, X. H. *Nat. Chem.* **2010**, *2*, 353–361.
- (15) Liu, Y. Z.; Hu, C. H.; Comotti, A.; Ward, M. D. *Science* **2011**, *333*, 436–440.
- (16) Icli, B.; Christinat, N.; Tonnemann, J.; Schuttler, C.; Scopelliti, R.; Severin, K. *J. Am. Chem. Soc.* **2009**, *131*, 3154–3155.
- (17) Jin, Y.; Voss, B. A.; Jin, A.; Long, H.; Noble, R. D.; Zhang, W. J. *Am. Chem. Soc.* **2011**, *133*, 6650–6658.
- (18) Yu, J.; Xu, R. *J. Mater. Chem.* **2008**, *18*, 4021–4030.
- (19) Yu, J.; Xu, R. *Acc. Chem. Res.* **2010**, *43*, 1195–1204.
- (20) Li, J. R.; Kuppler, R. J.; Zhou, H. C. *Chem. Soc. Rev.* **2009**, *38*, 1477–1504.
- (21) Liu, Y.; Xuan, W.; Cui, Y. *Adv. Mater.* **2010**, *22*, 4112–4135.
- (22) Lee, J. Y.; Farha, O. K.; Roberts, J.; Scheidt, K. A.; Nguyen, S. T.; Hupp, J. T. *Chem. Soc. Rev.* **2009**, *38*, 1450–1459.
- (23) Yoon, M.; Srirambalaji, R.; Kim, K. *Chem. Rev.* **2012**, *112*, 1196–1231.
- (24) Yuan, G.; Zhu, C.; Liu, Y.; Xuan, W.; Cui, Y. *J. Am. Chem. Soc.* **2009**, *131*, 10452–10460.
- (25) Zhang, J.; Chen, S. M.; Zingiryan, A.; Bu, X. H. *J. Am. Chem. Soc.* **2008**, *130*, 17246–17247.
- (26) Ma, L. Q.; Abney, C.; Lin, W. *Chem. Soc. Rev.* **2009**, *38*, 1248–1256.
- (27) Li, G.; Yu, W. B.; Ni, J.; Liu, T. F.; Liu, Y.; Sheng, E. H.; Cui, Y. *Angew. Chem., Int. Ed.* **2008**, *47*, 1245–1249.
- (28) Bradshaw, D.; Prior, T. J.; Cussen, E. J.; Claridge, J. B.; Rosseinsky, M. J. *J. Am. Chem. Soc.* **2004**, *126*, 6106–6114.
- (29) Wang, W.; Dong, X.; Nan, J.; Jin, W.; Hu, Z.; Chen, Y.; Jiang, J. *Chem. Commun.* **2012**, *48*, 7022–7024.
- (30) Seo, J. S.; Whang, D.; Lee, H.; Jun, S. I.; Oh, J.; Jeon, Y. J.; Kim, K. *Nature* **2000**, *404*, 982–986.
- (31) Nuzhdin, A. L.; Dybtsev, D. N.; Bryliakov, K. P.; Talsi, E. P.; Fedin, V. P. *J. Am. Chem. Soc.* **2007**, *129*, 12958–12959.
- (32) Padmanaban, M.; Muller, P.; Lieder, C.; Gedrich, K.; Grunker, R.; Bon, V.; Senkovska, I.; Baumgartner, S.; Opelt, S.; Paasch, S.; Brunner, E.; Glorius, F.; Klemm, E.; Kaskel, S. *Chem. Commun.* **2011**, *47*, 12089–12091.
- (33) Xie, S. M.; Zhang, Z. J.; Wang, Z. Y.; Yuan, L. M. *J. Am. Chem. Soc.* **2011**, *133*, 11892–11895.
- (34) Tanaka, K.; Muraoka, T.; Hirayama, D.; Ohnishi, A. *Chem. Commun.* **2012**, *48*, 8577–8579.
- (35) Cychosz, K. A.; Ahmada, R.; Matzger, A. J. *Chem. Sci.* **2010**, *1*, 293–302.
- (36) Sahoo, S. C.; Kundu, T.; Banerjee, R. *J. Am. Chem. Soc.* **2011**, *133*, 17950–17958.
- (37) Koh, L. L.; Ranford, J. O.; Robinson, W. T.; Svensson, J. O.; Tan, A. L. C.; Wu, D. Q. *Inorg. Chem.* **1996**, *35*, 6466–6472.
- (38) Mantina, M.; Chamberlin, A. C.; Valero, R.; Cramer, C. J.; Truhlar, D. G. *J. Phys. Chem. A* **2009**, *113*, 5806–5812.
- (39) Marenich, A. V.; Olson, R. M.; Kelly, C. P.; Cramer, C. J.; Truhlar, D. G. *J. Chem. Theory Comput.* **2007**, *3*, 2011–2033.
- (40) Nawrocki, J. J. *Chromatogr. A* **1997**, *779*, 29–71.
- (41) Hussain, M. D.; Saxena, V.; Brausch, J. F.; Talukder, R. M. *Int. J. Pharm.* **2012**, *422*, 290–294.
- (42) Adams, S. S.; Bresloff, P.; Mason, G. C. *J. Pharmac. Pharmacol.* **1976**, *28*, 256–257.
- (43) Maes, M.; Vermoortele, F.; Alaerts, L.; Couck, S.; Kirschhock, C. E. A.; Denayer, J. F. M.; De Vos, D. E. *J. Am. Chem. Soc.* **2010**, *132*, 15277–15285.
- (44) Millange, F.; Guillou, N.; Medina, M. E.; Ferey, G.; Carlin-Sinclair, A.; Golden, K. M.; Walton, R. I. *Chem. Mater.* **2010**, *22*, 4237–4245.
- (45) Comotti, A.; Bracco, S.; Sozzani, P.; Horike, S.; Matsuda, R.; Chen, J.; Takata, M.; Kubota, Y.; Kitagawa, S. *J. Am. Chem. Soc.* **2008**, *130*, 13664–13672.
- (46) Ferey, G.; Serre, C.; Devic, T.; Maurin, G.; Jobic, H.; Llewellyn, P. L.; DeWeireld, G.; Vimont, A.; Daturi, M.; Chang, J. S. *Chem. Soc. Rev.* **2011**, *40*, 550–562.